CAV18-05098

Fuel nozzle geometry effects on cavitation and spray behavior at diesel engine conditions

Brandon A. Sforzo*[1], Katarzyna E. Matusik[2], Christopher F. Powell[1], Alan L. Kastengren[2], Shane Daly[3], Scott Skeen[4], Emre Cenker[4], Lyle M. Pickett[4], Cyril Crua[5], and Julien Manin[6]

[1]*Energy Systems Division, Argonne National Laboratory, Argonne, IL 60439*
[2]*X-ray Science Division, Argonne National Laboratory, Argonne, IL 60439*
[3]*School of Mechanical, Industrial, and Manufacturing Engineering, Oregon State University, Corvallis, OR 97331*
[4]*Combustion Research Facility, Sandia National Laboratories, Livermore, CA 94550*
[5]*Advanced Engineering Centre, University of Brighton, Brighton BN2 4GJ, UK*
[6]*Artium Technologies, Inc., Sunnyvale, CA 94085*

Cavitation dynamics of diesel and gasoline injection nozzles has been a topic of ongoing research due to the effect of cavitation on the characteristics of the fuel spray, including the discharge coefficient, outlet velocity, spray angle, and atomization process. Additionally, repeated collapse of vapor cavities can damage nozzle surfaces, permanently changing the boundary conditions of the fluid flow field. Understanding the evolution and behavior of cavitation can therefore allow more precise control over its presence, as well as improved predictability of the corresponding fuel spray distribution.

Studies have shown that the inception and persistence of fuel vapor inside the spray hole is sensitive to geometric features of the injection nozzle, such as the degree of taper and inlet corner radius of curvature. For example, a hole with a cylindrical profile and sharp inlet corner more readily supports cavitation formation as compared to a monotonically converging hole with a rounded inlet. To better understand the effect of these geometric features on cavitation formation, and by extension, on the associated fuel spray, we compare the nozzle geometry and spray characteristics of two single-hole diesel injectors procured through collaboration with the Engine Combustion Network (ECN). The Spray C injector, specifically designed by the ECN for the express purpose of studying cavitating flows, features a cylindrical hole with a slight divergence near the outlet and a relatively sharp inlet corner. Its non-cavitating analog, the Spray D injector, contains a rounded inlet corner and a gently converging hole profile.

High-resolution x-ray tomography measurements coupled with optical microscopy images of both injectors provide the nozzle geometry with $\mathcal{O}(1)$ µm spatial resolution. Analysis of the measured geometries reveal that the radius of curvature of the hole inlet varies azimuthally for the modestly hydroground Spray C injector. To elucidate the effect that this asymmetric inlet condition has on cavitation formation during *operando* conditions, the fuel flow inside the nozzle hole was recorded using high-speed x-ray phase contrast imaging. These images reveal the formation of an asymmetric sheath of fuel vapor that persists throughout the injection event. Complementary x-ray and optical diagnostics of the downstream fuel spray further highlight the effect that this cavitation layer has on the spreading angle of the spray in comparison to the non-cavitating Spray D injector.

Keywords: fuel sprays; cavitation; x-ray tomography; x-ray radiography; long distance microscopy

Introduction

The study of geometry-induced cavitation in diesel fuel injection nozzles is motivated by its potentially damaging impact on the nozzle body as well as its influence on the fuel spray distribution, which in turn can affect the combustion emissions profile, performance, and fuel economy of a vehicle. The presence of cavitation has been associated with enhanced atomization, increased spreading angle, and decreased discharge of the fuel spray, to name a few effects [1–5]. Research dating back to the early 1960s has strived to understand the effect of nozzle orifice shape on the corresponding spray structure, largely focusing on simple geometries such as that of a plain-orifice nozzle [6–8]. Numerous experimental [9, 10] and numerical [11–13] works have demonstrated the importance of the inlet corner radius of curvature and hole conicity in dictating the onset of cavitation. It has also been shown that an asymmetric inlet condition, such as that of an angled nozzle, can create correspondingly asymmetric cavitation [10]. More complex geometries relevant to diesel injection have also been studied, including valve-covered orifice and sac-type, multi-hole nozzles [1, 14].

An ongoing challenge in the study of cavitation in diesel injectors is the ability to observe its formation and structure in the internal and near-nozzle region. Historically, transparent nozzles have been used as a proxy for diesel nozzles to study the flow structure optically, and have been designed out of materials such as acrylic or quartz, both of which offer an index of refraction that may be matched by the working fluid in order to reduce unwanted artifacts during visualization. Because such materials are somewhat pressure-limited, a compromise is made by creating large-scale

*Corresponding Author, Brandon Sforzo: bsforzo@anl.gov

Table 1: Summary of operating conditions for measuring the spray characteristics of ECN Spray C and Spray D.

Operating Condition	Diagnostic Technique		
	High-speed optical imaging	X-ray imaging	X-ray radiography
Ambient gas temperature (K)	440, 900	298	298
Ambient gas pressure (MPa)	2.9, 6	0.1, 0.2	2
Ambient gas density (kg m^{-3})	22.8	1.4	22.8
Ambient gas O_2 (%)	0	0	0
Fuel type	n-dodecane	n-dodecane	n-dodecane
Injection pressure (MPa)	150	150	150
Fuel temperature at nozzle (K)	440, 363	298	298
Hyd. injection duration (ms)	2.5	2.5	2.5

nozzles that can target Reynolds numbers relevant to diesel injection, albeit at lower injection pressure. However, there is evidence that scaling up the nozzle geometry while holding the Reynolds and cavitation numbers constant produces different cavitation structures [15]. To circumvent this scaling issue, nozzles manufactured from sapphire have been used due to the material's similarity in strength to steel and ability to withstand engine-relevant injection pressures [16].

Complementary to optical techniques, x-ray diagnostics can provide qualitative and quantitative measurements of in-hole cavitation as well as the near-nozzle spray structure. X-rays have the ability to penetrate through opaque material and only weakly refract from gas-liquid interfaces, making them ideal for probing optically thick regions of a spray [5]. The high flux and high energy x-ray synchrotron source of the Advanced Photon Source (APS) at Argonne National Laboratory has been used in the past to provide the requisite x-rays for measurements of the internal and near-nozzle flow structure of cavitating systems with micrometer spatial and microsecond temporal resolution using techniques such as radiography and fluorescence [17, 18]. In addition, x-ray phase contrast imaging has been previously implemented to obtain a qualitative understanding of the internal nozzle flow [19, 20]. This technique can be readily extended to actual-size diesel injectors operating at engine-relevant injection pressures.

In this paper, we leveraged both optical and x-ray diagnostic techniques to study the internal and near-nozzle flow of two single-hole diesel injectors, one of which strongly cavitates under typical diesel operating conditions. The injectors were obtained through the Engine Combustion Network (ECN) [21]. X-ray diagnostics were used to characterize the internal geometry and flow structure, as well as the near-nozzle spray distribution. Complementary optical diagnostics performed at Sandia National Laboratories extended the analysis of the spray structure to higher ambient and fuel temperatures. Previous comparison of x-ray radiography measurements and long-distance microscopy imaging of a diesel fuel spray has shown that the spray edge as defined by an optical thickness of unity corresponds to a projected fuel mass from the x-ray measurement on the order of 1 $\mu g/mm^2$ [22]. Provided with these thresholds, the spray angle as obtained through the x-ray radiography technique may be directly compared to that measured from long-distance microscopy imaging in order to explore the effect of cavitation on the jet width at variable operating conditions.

Experimental Methods

A suite of diagnostic techniques was implemented to characterize the internal geometry and spray behavior of two single-hole diesel injectors designated as Spray C #210037 and Spray D #209134 by the ECN. The target conditions used for each spray diagnostic technique are summarized in Table 1. When possible, the ECN-specified non-reacting operating conditions were utilized. Figure 1(a) illustrates the ECN coordinate system [23] convention used throughout this work. The injectors were measured from two viewing angles to explore potential asymmetries in the flow, designated as "View 1" and "View 2", corresponding to measurements taken in the X-Y plane and X-Z plane, respectively, with the origin at the nozzle tip.

Spray C and Spray D are common-rail fuel injectors fitted with two different single-hole nozzles that vary in diameter and shape. Spray D was designed to feature a relatively round hole inlet corner with a converging profile, and is intended to be the non-cavitating analog of Spray C, which, in contrast, underwent minimal hydro-erosion to help maintain a sharp inlet corner and a cylindrical hole profile.

To understand the effect of geometry on cavitation behavior, and by extension, the fuel spray distribution, high-resolution x-ray computed tomography (CT) scans of the injector geometries were obtained at the 7-BM beamline of the APS [24]. The nozzle geometry was reconstructed from a series of 2D projections using TomoPy [25]. The final spatial resolution of the geometry is 1.8 μm with a field of view (FOV) of 2.25 × 1.4 mm, capturing the full hole profile as well as part of the sac region. A more thorough discussion of the experimental setup, image processing, spatial uncertainty, and geometric analysis may be found in prior work [26].

Internal nozzle flow visualization for Spray C and Spray D was achieved with high speed x-ray phase contrast imaging conducted at the 32-ID-B beamline at APS, using similar methodology as in Ref. [19]. Visible light imaging of a scintillator was performed with a high-speed camera fitted with a 5× microscope objective, operated at 50,000 fps, gathering 250 frames per injection event repeated for 30-40 events. Spray C and Spray D imaging was performed with ambient pressures of 0.1 and 0.2 MPa, respectively.

Measurements of the time-resolved projected fuel density field were carried out at the 7-BM facility at APS using time-resolved x-ray radiography [24]. Each injector was horizontally mounted in a chamber that was pressurized to 2 MPa with N_2, which was also used to purge the environment at a flow rate of 4 standard L/min to inhibit droplet accumulation in the field of view during data acquisition. The injectors were driven by a common-rail light-duty diesel injection system, and triggered at a rate of 3 Hz for a commanded injection duration of 725 μs. The beam was focused to a 4 × 6 μm spot with the focal point aligned with the injector tip. The pressure chamber was translated over a grid to build a raster plot of measurement points, capturing the spray evolution up to 25 mm from the nozzle tip. The measured incident x-ray intensity at each spatial location was averaged over 16 injection events. X-ray photons undergo photoelectric absorption as they pass through the fuel spray, with the degree of absorption directly related to the line-of-sight density via the Beer-Lambert law [27]. The recorded beam intensity was binned over a single synchrotron orbit, providing a temporal resolution of 3.68 μs.

The fuel sprays were also injected in Sandia's optically-accessible vessel to gather high-speed microscopic images under varying fuel and ambient temperatures. High-speed images were collected at both View 1 and View 2 to ascertain the spray growth rate and transient development. At a typical View 2 condition, the camera operated at 40,000 fps, under an effective optical magnification of approximately 5.6× (digital scale factor = 5 μm/pix). Details of the experimental arrangement, and optical characterization are provided in Ref. [28].

Results

Figure 1(b) plots the radii as a function of axial distance for each of the injectors, revealing a smooth inlet corner and a monotonically converging hole profile for Spray D, both of which mitigate cavitation formation. In contrast, Spray C is characterized by a sharper inlet corner and diverging hole with a chamfer at the nozzle exit. The hole exit diameters have been verified with optical microscopy measurements performed at Sandia [29, 30].

The high spatial resolution of the geometry measurements allows the radius of curvature to be azimuthally resolved, revealing the existence of hole inlet curvature profiles that are known to influence the flowfield and encourage cavitation [10, 11]. Tomography reconstructions were processed along the hole inlet periphery in a similar manner as Ref. [31] to extract the radius of curvature as a function of the azimuthal angle, θ, as seen in figure 1(c). The more strongly hydroground Spray D injector maintains a relatively uniform radius of curvature of 112 ± 4 μm. In contrast, the hole inlet of Spray C is generally sharper and varies azimuthally, with a mean value of 41 ± 6 μm, and the sharpest edges near $\theta = 0^\circ$.

Phase contrast images were post-processed to highlight the signal contrast between internal fluid flow and fuel vapor during an injection event. Image sequences from the 30 to 40 injection events were ensemble-median-averaged to increase the level of signal-to-noise during the event. Figure 2 depicts the time-averages of the steady portion of each injection sequence. The processing method highlights all signal variation between the no-flow period and the steady injection phase; this includes motions of the injector, which manifest themselves as intensity variations at the sac and hole edges.

Cavitation presence can be seen clearly in figure 2(a) inside the top portion of the hole, which corresponds to the $\theta = 0^\circ$ location of the injector. This azimuthal location roughly corresponds to the hole entrance edge with the smallest radius of curvature. In contrast, the $\theta = 180^\circ$ location on the lower side of figure 2(a) shows no cavitation, which corresponds

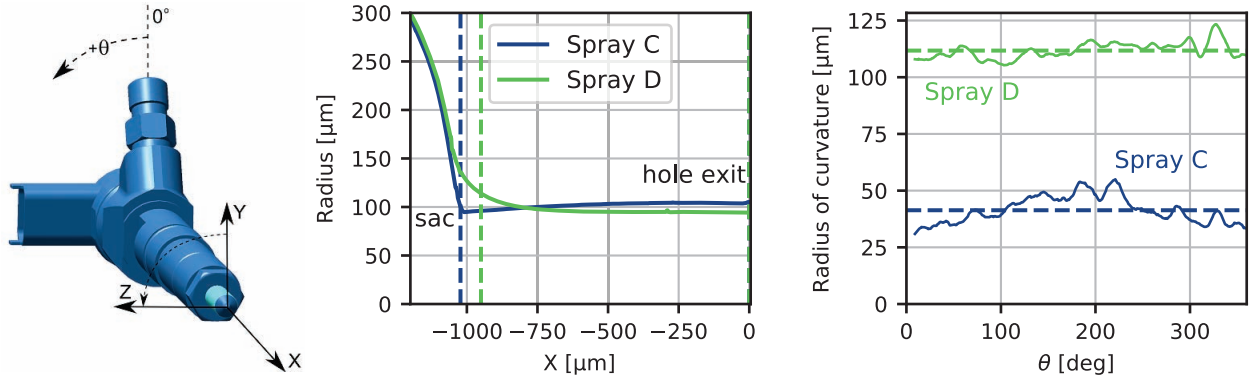

(a) Injector coordinates (b) Hole profiles (c) Inlet curvature

Figure 1: (a) ECN coordinate system for the Spray C and Spray D injectors. (b) Radial profiles of Spray C and Spray D injectors. The fuel enters from the sac and exits through the hole outlet. The vertical dashed lines indicate the start and end of each hole. (c) Hole inlet curvature as a function of azimuthal angle (θ) for Spray C and Spray D injectors. The dashed horizontal lines indicate the mean value.

to the smoothest edge of the hole entrance. The cavitation visible at the $\theta = 0°$ location grows rapidly from the entrance corner to a thickness of 47 μm at 200 μm downstream (X $= -825$ μm). This represents approximately 25% of the hole diameter. The thickness of the vapor sheath appears to asymptote by 600 μm downstream (X $= -425$ μm), to a thickness of 74 μm, corresponding to 38% of the hole diameter.

In figure 2(b), the orthogonal view depicts the presence of a thinner sheath on both the $\theta = 90°$ and 270° sides. At X $= -825$ μm, the sheath thicknesses from both sides are 27 and 23 μm, totaling to account for 26% of the hole diameter. Further downstream, the vapor regions thin to only 20% of the diameter by X $= -250$ μm. Unlike both views of the Spray C nozzle, neither view (figures 2(d) and 2(e)) of Spray D indicates any presence of cavitation. The edges of the geometry are highlighted due to vibrations caused by the needle motion. It can be deduced that at these operating conditions, and with a hole geometry that is cylindrical or divergent, the inception of cavitation is encouraged by the flow over a radius of curvature that is near or smaller than 40 μm.

Figures 2(c) and 2(f) display the steady-state projected density profiles of the fuel jet at X = 2 mm for Spray C and Spray D, respectively. Figure 2(c) clearly illustrates the asymmetric nature of the fuel distribution caused by the presence of cavitation inside the Spray C nozzle. The vapor sheath seen in figure 2(a) occludes a portion of the hole exit area, creating a unimodal spray profile that is skewed and wider in the +Y direction, while the peak projected mass shifts to the -Y direction. The projected density profile in View 2 instead reveals a bimodal distribution, where the value is lowest at the center. From this vantage, the integration line-of-sight passes normally to the thick vapor sheath interface, visible in figure 2(a), which has displaced the liquid away from the centerline. The downstream measurement, including those at axial X positions less than 2 mm, affirms that the sheath is thickest near the θ=0° location and this mass distribution propagates downstream.

Additionally, the profile from View 2, in figure 2(c), suggests that the region occluded by cavitation along the Y axis is thicker near +Z, as indicated by the lower projected mass for +Z in comparison to the peak near the -Z axis. Figure 2(f) suggests a more archetypal fuel spray distribution from Spray D, featuring a unimodal and relatively symmetric structure across both viewpoints. There is no indication in the phase-contrast images that cavitation is present in Spray D at the investigated conditions.

While the x-ray radiography profiles indicate asymmetry in distribution, this information is not typically known *a priori* for determining a threshold for optical characterization. However, previous research has shown that using a low threshold for projected mass (1 $\mu g/mm^2$) is comparable to an optical thickness of unity [22]. Therefore, a radiography full jet width was determined by setting a threshold on the steady-state projected density profile and locating the two points on the tails of the distribution. This definition of jet width actually indicates a wider Spray C at View 1 than at View 2 (0.50 mm vs. 0.47 mm, respectively) even though View 2 appears wider at higher projected mass values.

Confirming this trend, the optical microscopy measurements shown in Figure 3 also show a wider Spray C for View 1 compared to View 2, including axial distances extending to 5 mm, while Spray D is rather symmetric. Note that

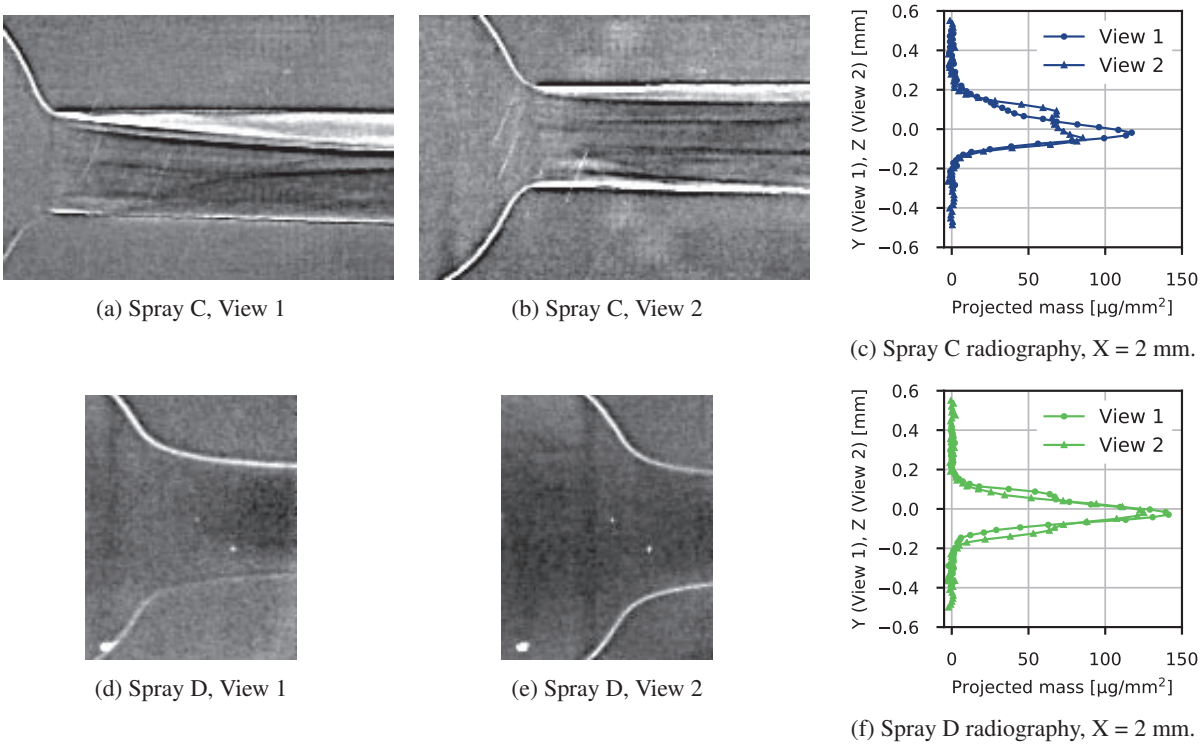

(a) Spray C, View 1

(b) Spray C, View 2

(c) Spray C radiography, X = 2 mm.

(d) Spray D, View 1

(e) Spray D, View 2

(f) Spray D radiography, X = 2 mm.

Figure 2: Phase contrast images of the steady-state internal flow for each view of the two injectors with paired radiography profiles at X = 2 mm downstream from the nozzle tips.

the optical liquid jet width depends upon the ambient and fuel temperature, becoming thinner with increased ambient temperature. Heated fuel temperature also tends to decrease spray width, though, only at increased ambient temperatures. For vaporization controlled by mixing, an increase in ambient and fuel temperature effectively increases the fuel concentration where liquid fuel exists, thereby decreasing the measured liquid jet width [32].

By comparing the measured jet width at several different ambient and fuel temperatures, the optical diagnostic exhibits a sensitivity to the distribution of fuel at low concentrations at the periphery of the spray, regions that are essentially in the noise floor of the radiography measurement. While the low-temperature (440 K) optical jet widths are larger than that of radiography at X = 2.0 mm, the high-temperature (900 K) jet widths are in closer agreement.

Unlike Spray D, the discrepancy in Spray C liquid jet width between the two viewpoints remains significant, suggesting that the impact of asymmetric cavitation existing inside the nozzle is propagated to the radial dispersion characteristics of the jet for a wide range of ambient temperatures, up to engine-relevant conditions. This suggests that as the fuel jet travels downstream, the presence of asymmetric cavitation is increasing the radial dispersion of low-density fuel in a likewise asymmetric fashion, i.e. cavitation is promoting rapid mixing and jet growth, but it occurs preferentially along the spray periphery and it is particularly aligned with the sharp inlet of the nozzle. A wider spreading angle for Spray C in comparison to Spray D at View 1 has been previously reported at ECN (900 K) conditions, including an impact on spray combustion processes [33].

Conclusions

This work investigated the influence of asymmetric injector nozzle geometry on the occurrence of cavitation and the resulting effect on fuel spray behavior at engine-like conditions. Optical and x-ray diagnostic techniques were used to investigate the internal and near-nozzle flow of two single-hole diesel injectors, Spray C and Spray D. The internal geometry of both injectors was measured with 1.8 μm spatial resolution, revealing sharp, asymmetric hole inlet contours in Spray C and a smoother and consistent curvature in Spray D. The location of the sharpest inlet feature in the Spray C geometry corresponded directly to cavitation during operation, visible through x-ray phase contrast

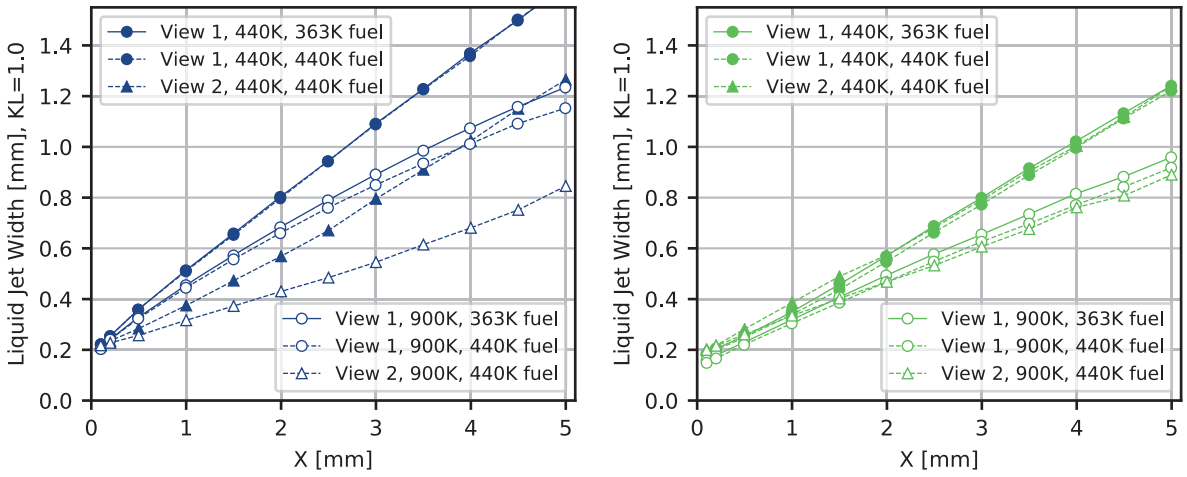

(a) Spray C (b) Spray D

Figure 3: Liquid fuel jet width as a function of axial distance from the injector tip measured using high-speed optical imaging. Note: Spray C, View 1, 440 K ambient data overlap.

imaging, with little to no cavitation observed at locations of smoother hole entrance curvature. Cavitation was not observed in Spray D. The presence of cavitation influenced the resulting fuel spray structure, with a bias of mass away from the region of cavitation near the nozzle exit (X = 0.1 mm). Spray C profiles at X = 2 mm indicate a widening of the spray in the measurement plane with cavitation, and overall wider spray angles than Spray D, indicating increased atomization resulting in regions of low-density fuel at the periphery. Spray widening due to cavitation was also observed through optical microscopy with little influence of fuel temperature at low ambient temperatures. At higher ambient temperatures, the width decreases non-uniformly between the two perspectives, indicating a sensitivity of the spray to cavitation. This discrepancy suggests that the impact of asymmetric cavitation inside the nozzle is propagated to the radial dispersion characteristics of the jet for a wide range of ambient temperatures, up to engine-relevant conditions. These observations illustrate the influence cavitation has on fuel spray behavior and thus the significance to engine performance. Furthermore, this cavitation influence and the coupling to the asymmetric geometry impresses the importance of inclusion of these factors in predictive models for fuel spray behavior.

Acknowledgements

Research presented in this paper was performed at the 7-BM and 9-ID beamlines at the Advanced Photon Source at Argonne National Laboratory. Use of the APS is supported by the U.S. Department of Energy (DOE) under Contract No. DEAC0206CH11357. Sandia National Laboratories is a multi-mission laboratory managed and operated by National Technology and Engineering Solutions of Sandia, LLC., a wholly owned subsidiary of Honeywell International, Inc., for the U.S. Department of Energys National Nuclear Security Administration under contract DE-NA0003525. The Argonne and Sandia fuel spray research is sponsored by the DOE Vehicle Technologies Program under the direction of Gurpreet Singh and Michael Weismiller.

References

[1] Soteriou, C., Andrews, R., and Smith, M., "Direct injection diesel sprays and the effect of cavitation and hydraulic flip on atomization," *SAE Technical Paper*, 1995.

[2] Tamaki, N., Shimizu, M., Nishida, K., and Hiroyasu, H., "Effects of cavitation and internal flow on atomization of a liquid jet," *Atomization and Sprays*, Vol. 8, 1998, pp. 179–197.

[3] Sou, A., Hosokawa, S., and Tomiyama, A., "Effects of cavitation in a nozzle on liquid jet atomization," *Int. J. Heat and Mass Transfer*, Vol. 50, 2007, pp. 3575–3582.

[4] Suh, H. K. and Lee, C. S., "Effect of cavitation in nozzle orifice on the diesel fuel atomization characteristics," *Int. J. Heat and Fluid Flow*, Vol. 29, 2008, pp. 1001–1009.

[5] Sou, A., Minami, S., Prasetya, R., Pratama, R., Moon, S., Wada, Y., and Yokohata, H., "X-ray visualization of cavitation in nozzles with various sizes," *ICLASS 2015, 13th Triennial International Conference on Liquid Atomization and Spray Systems*, 2015.

[6] Bergwerk, W., "Flow pattern in diesel nozzle spray holes," *Proceedings of the Institution of Mechanical Engineers*, Vol. 173, No. 1, 1959, pp. 655–660.

[7] Hall, G. W., "Analytical determination of the discharge characteristics of cylinder-tube orifices," *Journal of Mechanical Engineering Science*, Vol. 5, No. 1, 1963.

[8] Nurick, W. H., "Orifice cavitation and its effect on spray mixing," *Journal of Fluids Engineering*, 1976, pp. 681–687.

[9] Ohrn, T., Senser, D., and Lefebvre, A., "Geometrical effects on discharge coefficients for plain-orifice atomizers," *Atomization and Sprays*, Vol. 1, No. 2, 1991, pp. 137–153.

[10] Chaves, H. and Ludwig, C., "Characterization of cavitation in transparent nozzles depending on the nozzle geometry," *Proceedings of the 20th ILASS-Europe Meeting 2005*, 2005.

[11] Schmidt, D. P., Rutland, C., Corradini, M., Roosen, P., and Genge, O., "Cavitation in two-dimensional asymmetric nozzles," *SAE Technical Paper*, 1999.

[12] Giannadakis, E., Papoulias, D., Gavaises, M., Arcoumanis, C., Soteriou, C., and Tang, W., "Evaluation of the predictive capability of diesel nozzle cavitation models," *SAE Technical Paper*, 2007.

[13] Som, S., Ramirez, A., Longman, D., and Aggarwal, S., "Effect of nozzle orifice geometry on spray, combustion, and emission characteristics under diesel engine conditions," *Fuel*, Vol. 90, 2011, pp. 1267–1276.

[14] Schmidt, D., Rutland, C., and Corradini, M., "A fully compressible, two–dimensional model of small, high-speed, cavitating nozzles," *Atomization and Sprays*, Vol. 9, 1999, pp. 255–276.

[15] Arcoumanis, C., Flora, H., Gavaises, M., and Badami, M., "Cavitation in real-size multi-hole diesel injector nozzles," *SAE Technical Paper*, 2000.

[16] Falgout, Z. and Linne, M., "Cavitation inside high-pressure optically transparent fuel injector nozzles," *Journal of Physics: Conference Series*, Vol. 656, 2015.

[17] Duke, D. J., Kastengren, A. L., Swantek, A. B., Matusik, K. E., and Powell, C. F., "X-ray fluorescence measurements of dissolved gas and cavitation," *Exp. Fluids*, Vol. 57, No. 162, 2016.

[18] Duke, D. J., Matusik, K. E., Kastengren, A. L., Swantek, A. B., Sovis, N., Payri, R., Viera, J. P., and Powell, C. F., "X-ray radiography of cavitation in a beryllium alloy nozzle," *Int. J. Eng. Research*, Vol. 18, No. 1-2, 2017.

[19] Duke, D., Swantek, A., Tilocco, Z., Kastengren, A., Fezzaa, K., Neroorkar, K., Moulai, M., Powell, C., and Schmidt, D., "X-ray Imaging of Cavitation in Diesel Injectors," *SAE Int. J. Engines*, Vol. 7, No. 2, 2014, pp. 1003–1016.

[20] Duke, D., Swantek, A., Kastengren, A., Fezzaa, K., and Powell, C., "Recent developments in x-ray diagnostics for cavitation," *SAE Int. J. Fuels Lubr.*, Vol. 8, No. 1, 2015.

[21] Pickett, L., "Engine Combustion Network," May 2014.

[22] Pickett, L. M., Manin, J., Kastengren, A., and Powell, C., "Comparison of near-field structure and growth of a diesel spray using light-based optical microscopy and x-ray radiography," *SAE Int. J. Engines*, Vol. 7, No. 2, 2014.

[23] Sandia National Laboratories, "Engine Combustion Network "Spray A" injector nozzle geometry," Accessed March 14, 2017.

[24] Kastengren, A., Powell, C., Arms, D., Dufresne, E., Gibson, H., and Wang, J., "The 7BM beamline at the APS: a facility for time-resolved fluid dynamics measurements," *J Synchrotron Rad*, Vol. 19, 2012, pp. 654–657.

[25] Gürsoy, D., Carlo, F. D., Xiao, X., and Jacobsen, C., "TomoPy: a framework for the analysis of synchrotron tomographic data," *J Synchrotron Rad*, Vol. 21, 2014, pp. 1188–1193.

[26] Matusik, K. E., Duke, D. J., Kastengren, A. L., Sovis, N., Swantek, A. B., and Powell, C. F., "High-resolution X-ray tomography of engine combustion network diesel injectors," *International Journal of Engine Research*, Vol. 0, No. 0, 2017.

[27] Als-Nielsen, J. and McMorrow, D., *Elements of modern x-ray physics*, chap. 9, John Wiley and Sons, 2011, pp. 307–313.

[28] Crua, C., Manin, J., and Pickett, L. M., "On the transcritical mixing of fuels at diesel engine conditions," *Fuel*, Vol. 208, No. Supplement C, 2017, pp. 535 – 548.

[29] Sandia National Laboratories, "Engine Combustion Network "Spray C" Injector Nozzle Geometry," 2016, Accessed July 22, 2016.

[30] Payri, R., Gimeno, J., Cuisano, J., and Arco, J., "Hydraulic characterization of diesel engine single-hole injectors," *Fuel*, Vol. 180, 2016, pp. 357 – 366.

[31] Kastengren, A., Tilocco, F., Powell, C., Manin, J., Pickett, L., Payri, R., and Bazyn, T., "Engine Combustion Network (ECN): measurements of nozzle geometry and hydraulic behavior," *Atomization and Sprays*, Vol. 22, No. 12, 2012, pp. 1011–1052.

[32] Siebers, D. L., "Scaling liquid-phase fuel penetration in diesel sprays based on mixing-limited vaporization," *SAE Technical Paper*, 1999.

[33] Westlye, F. R., Battistoni, M., Skeen, S. A., Manin, J., Pickett, L. M., and Ivarsson, A., "Penetration and combustion characterization of cavitating and non-cavitating fuel injectors under diesel engine conditions," *SAE Technical Paper*, 2016.